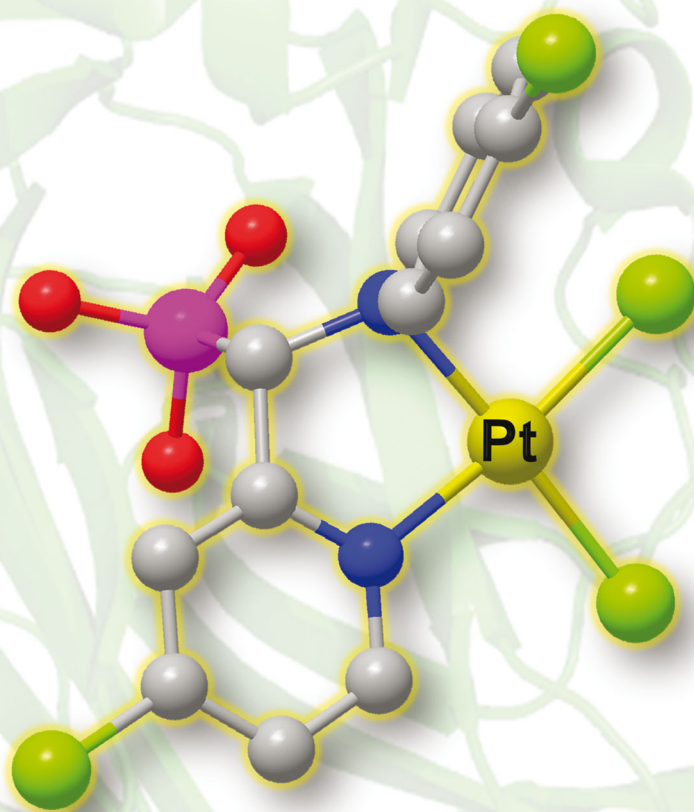


# ChemComm

Chemical Communications

rsc.li/chemcomm

Ca<sup>2+</sup>



ISSN 1359-7345



ROYAL SOCIETY  
OF CHEMISTRY

Celebrating  
IYPT 2019

## COMMUNICATION

Taotao Zou, Zhen-Feng Chen, Hong Liang *et al.*  
An aminophosphonate ester ligand-containing platinum(II)  
complex induces potent immunogenic cell death *in vitro*  
and elicits effective anti-tumour immune responses *in vivo*


 Cite this: *Chem. Commun.*, 2019, 55, 13066

 Received 23rd August 2019,  
 Accepted 23rd September 2019

DOI: 10.1039/c9cc06563f

rsc.li/chemcomm

# An aminophosphonate ester ligand-containing platinum(II) complex induces potent immunogenic cell death *in vitro* and elicits effective anti-tumour immune responses *in vivo*†

 Ke-Bin Huang,<sup>‡</sup> Feng-Yang Wang,<sup>‡</sup> Hai-Wen Feng,<sup>a</sup> Hejiang Luo,<sup>c</sup> Yan Long,<sup>c</sup> Taotao Zou,<sup>‡</sup> Albert S. C. Chan,<sup>c</sup> Rong Liu,<sup>a</sup> Huahong Zou,<sup>a</sup> Zhen-Feng Chen,<sup>\*a</sup> Yan-Cheng Liu,<sup>a</sup> You-Nian Liu<sup>b</sup> and Hong Liang<sup>‡</sup>

**A platinum(II) complex containing an aminophosphonate ligand preferentially accumulates in the endoplasmic reticulum (ER) in association with potent ER stress and reactive oxygen species generation, followed by the activation of damage-associated molecular pattern signals and immune responses. Importantly, the Pt complex exhibits potent anti-tumour activities in two independent mouse models via an immunogenic cell death pathway.**

Cisplatin and its derivatives have received worldwide attention in clinical cancer treatment.<sup>1–4</sup> Their mechanisms of action are considered to involve DNA binding *via* forming Pt-guanine adducts in association with downstream DNA damage and strand break-mediated apoptosis.<sup>5,6</sup> Besides directly killing cancer cells, oxaliplatin, the third-generation cisplatin analogue, has been reported to induce immunogenic cell death (ICD) by activating innate and adaptive immune responses, which is likely caused by targets other than DNA.<sup>7,8</sup> The tumour-specific immune responses evoked by ICD inducers endow a “second hit” to the residual cancer cells which were not killed by the original drug cytotoxicity.<sup>9–11</sup> As a result, a long-term therapeutic benefit from ICD may be possible.<sup>12–15</sup> This has inspired a growing interest to develop more promising ICD-inducing complexes.<sup>16–18</sup> Unfortunately, the last 10 years witnessed very slow advances in developing novel ICD

complexes. Only a handful of metal-based ICD compounds have been reported, including a luminescent cyclometallated Pt complex,<sup>19</sup> KP1019,<sup>20</sup> and a Pt(IV) prodrug containing an oxaliplatin framework.<sup>21</sup>

Many calcium storage proteins, including calreticulin (CRT), are localized in the ER which thus carries a high concentration of Ca<sup>2+</sup>; disruption of calcium homeostasis has been reported to cause ER stress and to promote CRT exposure to the cell membrane, which serves as an “eat me” signal to be recognized by phagocytic dendritic cells, subsequently eliciting other immune cells to respond.<sup>22–24</sup> Phosphate/phosphonate-containing compounds are known to possess mineral calcium-targeting properties<sup>25–27</sup> and are able to alter calcium trafficking in cells.<sup>28</sup> As many labile Pt(II) complexes are able to induce ROS,<sup>29,30</sup> we assume that the Pt(II) complexes bearing an aminophosphonate ligand could potentially trigger ICD through ER targeting and ROS generation.<sup>31,32</sup> Herein we report a novel platinum(II) complex containing an aminophosphonate ester ligand displaying a lipophilicity amenable to bioactivity and inducing potent ER stress accompanied by ROS generation, subsequently triggering immunogenic responses that kill cancer cells. Importantly, the Pt complex displays a low acute toxicity while effectively suppressing tumour growth in a vaccination mouse model and a tumour-bearing mouse model.

We synthesized 12 novel aminophosphonate–platinum(II) complexes (Fig. 1) with full characterization by <sup>1</sup>H NMR, ESI-MS and elemental analysis (see details in the synthesis section and Fig. S1 and S2, ESI†). We also performed X-ray crystallography on 9 complexes (Fig. S3 and Table S1 in ESI†). The three types of complexes differ in the number of CH<sub>2</sub> units between the benzene ring and the imide that coordinates to the Pt center. These Pt complexes are well dissolved in common organic solvents such as DMF and DMSO and are soluble in PBS after dilution from DMSO stock solution (1% DMSO unless otherwise stated<sup>33</sup>). The stability test by HPLC demonstrated that the Pt complexes are stable for 48 h at room temperature under physiological conditions (Tris–KCl–HCl buffer, pH 7.35, Fig. S4, ESI†).

<sup>a</sup> State Key Laboratory for Chemistry and Molecular Engineering of Medicinal Resources, School of Chemistry & Pharmacy, Guangxi Normal University, Guilin, Guangxi, 541004, P. R. China. E-mail: chenzf@gxnu.edu.cn, hliang@gxnu.edu.cn

<sup>b</sup> College of Chemistry and Chemical Engineering, Central South University, Changsha, Hunan 410083, P. R. China

<sup>c</sup> Guangdong Key Laboratory of Chiral Molecule and Drug Discovery, School of Pharmaceutical Science, Sun Yat-sen University, Guangzhou 510006, China. E-mail: zoutt3@mail.sysu.edu.cn

<sup>d</sup> School of Science and Engineering, The Chinese University of Hong Kong, Shenzhen 518172, China

† Electronic supplementary information (ESI) available: Synthesis and characterization of complexes, procedures for ICD-related experiments and supporting figures. CCDC 1542728–1542736. For ESI and crystallographic data in CIF or other electronic format see DOI: 10.1039/c9cc06563f

‡ These authors contributed equally.

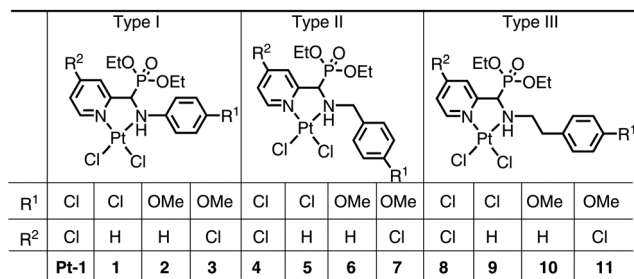


Fig. 1 chemical structures of the Pt(II) complexes. The racemic mixtures were used for biological studies.

The complexes generally display cytotoxicity against different cancer cells, including urinary bladder transitional cell carcinoma (T-24), bone osteosarcoma (MG-63), hepatocellular carcinoma (HepG2), and ovarian cancer (SK-OV-3), with IC<sub>50</sub> ranging from 0.25–88.7 μM in a 48 h treatment (Table S2, ESI<sup>†</sup>). These values are generally smaller than that in normal human liver cells (HL-7702). As shown in Table S2 (ESI<sup>†</sup>), the cytotoxicity is decreased by lowering the lipophilicity from –Cl, to –H to –OMe substituents for the same type of complexes. Additionally, the electron-inductive effects play a rather important role: the presence of an electron-withdrawing –Cl moiety at the *para*-position of aniline (**Pt-1**, **1**) or pyridine (**Pt-1**, **3**) significantly improves the cytotoxicity whereas the electron-donating –OMe moiety adversely decreases the cytotoxicity (**2**, **3**). Complex **Pt-1**, in which the aminophosphonate-pyridine ligand contains two Cl atoms that are most electron-withdrawing and are most lipophilic, exhibits the highest cytotoxicity against cancer cells and the largest fold-difference (>50-fold) compared to normal cells. For comparison, the aminophosphonate-pyridine ligand displays a much lower cytotoxicity (Fig. S5, ESI<sup>†</sup>). Since the Pt complexes display strong cytotoxicity against bladder transitional cell carcinoma that are also suitable to establish immune tumour models, bladder cancer cells were used in the following biological activity studies.

To examine whether the phosphonate ester is hydrolysed *in vitro*, we incubated T-24 cells with **Pt-1** for 24 h. The ESI-MS analysis of the supernatant after ethanol precipitation of cell lysates showed the presence of mono- and bi-hydrolyzed phosphonate with one Pt–Cl bond hydrolysis (Fig. S6, ESI<sup>†</sup>). The ICP-MS of subcellular fractions from **Pt-1**-treated T-24 cells after 24 h (Fig. S7, ESI<sup>†</sup>) shows a major localization of the complex to the ER (2.20 ± 0.18 ng Pt per million cells) over the mitochondria (0.80 ± 0.26) and nucleus (0.94 ± 0.15). This ER accumulation may be attributed to the ER's high concentration of Ca<sup>2+</sup>, which has a high affinity for phosphonate.<sup>25</sup> By Western blot analysis, we observed a protein profile characteristic of ER stress, including the expression of phosphorylated protein kinase RNA-like endoplasmic reticulum kinase (PERK), phosphorylated eukaryotic initiation factor 2α (eIF2α), and C/EBP homologous protein (CHOP), in T-24 cells treated at an IC<sub>50</sub> concentration (0.5 μM) of **Pt-1** for 48 h (Fig. S8, ESI<sup>†</sup>). This treatment is also associated with a time-dependent increase in ROS, as indicated by 2',7'-dichlorodihydro-fluorescein diacetate (DCFH) staining (Fig. S9, ESI<sup>†</sup>).

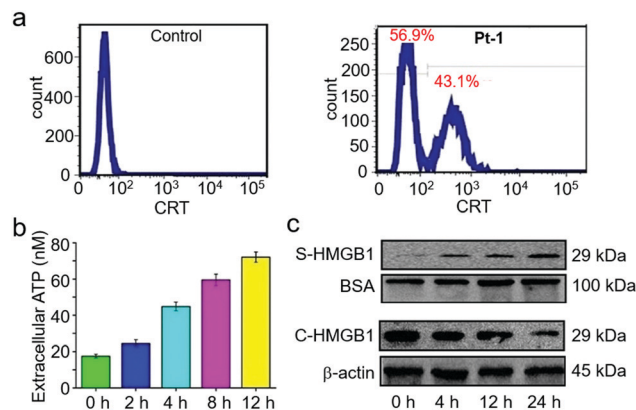
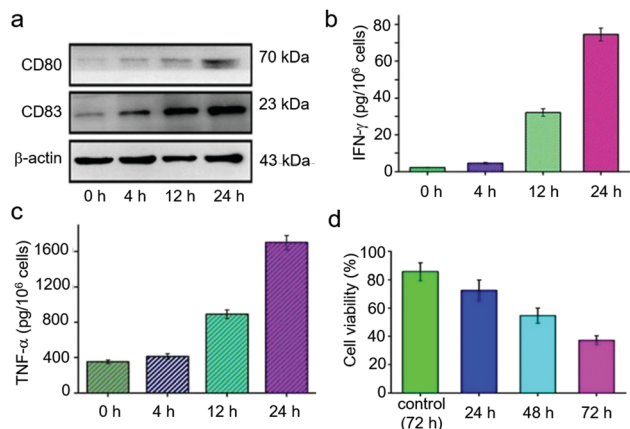


Fig. 2 The activation of DAMPs in T-24 cells after **Pt-1** treatment. (a) Flow cytometry analysis of CRT on the surface of T-24 cells treated with solvent control or 0.5 μM **Pt-1** for 2 h. (b) The ATP concentration in culture medium after treating T-24 cells with 0.5 μM of **Pt-1** as measured by luciferase assay. (c) Levels of HMGB1 in culture medium (S-HMGB1) and in cells (C-HMGB1) after incubating T-24 cells with 0.5 μM of **Pt-1**.

Conditions of stress can stimulate damage-associated molecular patterns (DAMPs) that recruit immune cells.<sup>13</sup> We treated T-24 cells with 0.5 μM **Pt-1** and labelled non-permeabilized cells with an anti-CRT antibody. Fluorescence microscopy revealed an intense immunofluorescence distributed in uneven clusters on the undamaged cell surface after 2 h (Fig. S10, ESI<sup>†</sup>), while in the control group without **Pt-1** treatment, no immunofluorescence was detected. This elevated surface immunofluorescence intensity is confirmed by flow cytometry experiments, in which 43.1% of treated cells displayed a higher fluorescence intensity than the control group (Fig. 2a). As anticipated, secretion of HMGB1 and ATP, another two DAMP signals, was clearly evident (Fig. 2b and c). A firefly luciferase assay reveals a time-dependent ATP secretion of up to 72.1 nM in the culture medium after 12 h treatment with **Pt-1**. Also, a gradual increase in secreted HMGB1 (S-HMGB1) was found by Western blot analysis in the culture medium after treating T-24 cells with 0.5 μM **Pt-1** for 24 h. This was accompanied by a time-dependent reduction in cellular HMGB1 (C-HMGB1). While under similar conditions, cisplatin did not obviously elicit these DAMP signals (Fig. S11, ESI<sup>†</sup>).

To study the effects of **Pt-1**-induced DAMPs on immune activity, we treated T-24 cancer cells with 0.5 μM **Pt-1** for 48 h, and used the cell-conditioned-culture medium (supernatant) to test its effects on immune cells.<sup>10</sup> We first examined the activity on the maturation of dendritic cells, since mature dendritic cells (mDCs) are one of the major antigen presenting cells.<sup>34</sup> The imDCs isolated from human peripheral blood mononuclear cells (PBMCs) were incubated with **Pt-1**-treated cell-conditioned culture medium. Western blot analysis (Fig. 3a) revealed an increased expression of the DC maturation marker, CD83, on the surface of non-permeabilized DCs after 4 h, which gradually increased after 12 and 24 h. The surface expression of CD80, another important DC maturation marker, exhibited a similar trend.<sup>12</sup> We next assessed the extracellular levels of the proinflammatory cytokines IFN-γ and TNF-α, both of which are critical for innate and adaptive immunity.<sup>13</sup> As shown in Fig. 3b and c, the **Pt-1**-treated



**Fig. 3** The induction of immune responses in PBMCs: (a) Expression of CD80 and CD83 on the surface of imDCs incubated with **Pt-1**-treated T-24 cell-conditioned culture supernatant for the indicated time. (b and c) Secretion of (b) IFN- $\gamma$  and (c) TNF- $\alpha$  from human primary PBMCs after incubation with **Pt-1**-treated T-24 cell-conditioned culture supernatants for the indicated time. (d) The average cell viability (%) of T-24 cells after treating with the activated PBMCs for the indicated time.

cell-conditioned culture medium boosted the IFN- $\gamma$  secretion from 2.1 pg at 0 h to 74.5 pg at 24 h per  $10^6$  PBMC cells (35-fold) and the TNF- $\alpha$  from 350 pg at 0 h to 1700 pg at 24 h per  $10^6$  PBMC cells (4.8-fold). However, incubating PBMCs with cell-conditioned culture medium without **Pt-1** treatment only led to the basal cytokine secretion (data not shown). Then the cytotoxicity of activated PBMCs was tested by MTT assay according to the literature procedure.<sup>35</sup> PBMCs pre-treated with the conditioned culture supernatants suppressed the tumour cell viability to 72.5% after 24 h and further decreased to 54.6% and 37.1% after 48 h and 72 h treatment, respectively (Fig. 3d); while the control group, which was co-incubated for 72 h with PBMCs treated with cancer cell-conditioned medium without drug treatment, showed a basal cytotoxicity with a mean cell viability of 85.6%. These results collectively indicate that the **Pt-1**-treated conditioned culture medium activates an immune response in PBMCs to kill cancer cells.

To examine the putative immunogenicity of exposed DAMPs from **Pt-1** *in vivo*, a syngeneic MB-49 mouse urothelial carcinoma tumour vaccination model was established.<sup>36</sup> The ICD inducer, oxaliplatin, which has been shown to be effective in urothelial cancer patients,<sup>37</sup> was used as a control. In general, MB-49 cells were treated with **Pt-1** (0.5  $\mu$ M) or oxaliplatin (1.3  $\mu$ M), or with solvent only for 48 h, and then the treated cells were injected (s.c.) into the left flanks of C57BL/6 mice ( $n = 10$  in each group) as a tumour vaccine. After 7 days, these mice were re-challenged in the opposite flanks by inoculation with untreated MB-49 cells (Fig. 4). The formation of tumours in the right flanks was then monitored every day for 35 days. In the solvent control group, tumours were found in 20% of mice 7 days after re-challenging, and 90% of mice in this group were detected with a tumour in the right flank after 10 days. While in the oxaliplatin and **Pt-1** treatment group, tumour development was significantly delayed from the second inoculation (Fig. 4). One mouse was found to carry a tumour at day 11 in the oxaliplatin group and the first mouse with a tumour

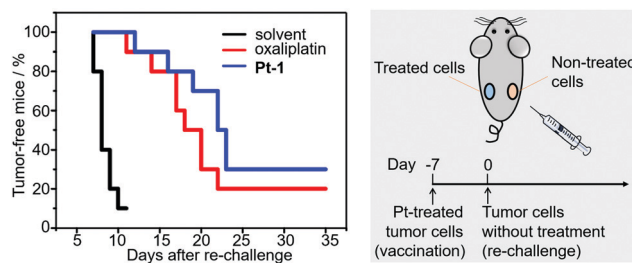


**Fig. 4** Anti-tumour vaccination. MB-49 cells were firstly treated with **Pt-1** (0.5  $\mu$ M), oxaliplatin (1.3  $\mu$ M) or solvent control for 48 h; then the treated MB-49 cells were subcutaneously injected into the left flanks of C57BL/6 mice ( $n = 10$ ), which were then re-challenged in the right flanks with untreated MB-49 cells 7 days later. Percentage of tumour-free mice after re-challenging with MB-49 cells was shown.

in the **Pt-1** group was identified at day 12. Gradually more tumour-bearing mice were identified by oxaliplatin treatment and reached a stable stage of 20% tumour-free mice after 22 days. Complex **Pt-1** displayed a slightly slower rate of tumour formation than oxaliplatin with a stable stage of 30% tumour-free mice after 23 days. The significantly delayed tumour formation suggests an activation of immunity to prevent tumour formation at a distant site.<sup>7,16</sup>

We further tested the ability of **Pt-1** to inhibit tumour growth in an immunocompetent mouse model. We initially examined the acute toxicity in C57BL/6 mice. **Pt-1** or oxaliplatin was administered (i.v.) at the doses shown in Table S3 (ESI<sup>†</sup>). In the oxaliplatin treatment group, one of the three mice died at 20  $\mu$ mol  $\text{kg}^{-1}$  (8 mg  $\text{kg}^{-1}$ ), and the rest of the mice were found dead at doses higher than 30  $\mu$ mol  $\text{kg}^{-1}$  (12 mg  $\text{kg}^{-1}$ ). In contrast, all mice survived **Pt-1** doses of 30  $\mu$ mol  $\text{kg}^{-1}$  (20 mg  $\text{kg}^{-1}$ ), demonstrating a significantly lower acute toxicity of **Pt-1** than oxaliplatin.

When the tumour volumes of C57BL/6 mice inoculated with MB-49 cells reached  $\sim 60 \text{ mm}^3$  ( $n = 5$  per group), an equimolar concentration of oxaliplatin (6 mg  $\text{kg}^{-1}$ ) or **Pt-1** (9.8 mg  $\text{kg}^{-1}$ ) was administered (i.v.) once every two days. As shown in Fig. 5a, **Pt-1** significantly suppresses tumour growth with a 59.6% inhibition compared to the solvent control ( $p < 0.001$ ) after 18 days. The inhibition by **Pt-1** is more potent than oxaliplatin which elicited a 49.2% inhibition after 18 days ( $p < 0.01$ ). No death or body weight loss was detected during the treatment (Fig. S12, ESI<sup>†</sup>).

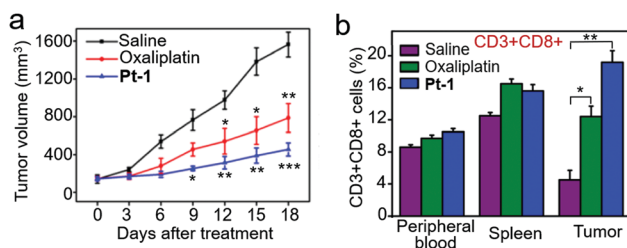


**Fig. 5** The induction of anti-tumour immune responses *in vivo*: (a) Tumour volumes of C57BL/6 mice bearing MB-49 cells ( $n = 5$ ) after treatment with 9.8 mg  $\text{kg}^{-1}$  **Pt-1** or 6 mg  $\text{kg}^{-1}$  oxaliplatin. (b) Percentage of cytotoxic CD3<sup>+</sup>CD8<sup>+</sup> T lymphocytes in the total cells isolated from peripheral blood, spleen, and tumours of C57BL/6 mice treated with **Pt-1** or oxaliplatin. \* $p < 0.05$ , \*\* $p < 0.01$ , \*\*\* $p < 0.001$ .

Then the amounts of CD3<sup>+</sup> T cells and CD3<sup>+</sup>CD8<sup>+</sup> T cells in the peripheral blood, spleen and tumours of C57BL/6 mice after 18 day treatment were determined.<sup>10</sup> We observed no change in the total CD3<sup>+</sup> proportions in peripheral blood, while a slight increase in the spleen and tumours was detected compared to the solvent control (Fig. S13, ESI<sup>†</sup>). The number of CD3<sup>+</sup>CD8<sup>+</sup> T lymphocytes in the peripheral blood and spleen slightly increases after treatment (Fig. 5b); notably, the proportions of CD3<sup>+</sup>CD8<sup>+</sup> cytotoxic T lymphocytes in tumour tissues were significantly increased from 6.5% of total cells in the solvent group to 20.7% in the Pt-1 treatment group, which is higher than that of the oxaliplatin group (16.4%). These results provide further support that Pt-1 can activate the immune system to alleviate cancer, with a higher activity than oxaliplatin.

In summary, platinum(II) complexes containing phosphonate esters were found to preferentially accumulate in the ER followed by ROS-associated ER stress, which triggers the exposure CRT on the cell membrane and the secretion of ATP and release of HMGB1. These DAMP signals primed the immune cells and cause cytotoxicity towards cancer cells. The gold-standard *in vivo* vaccination assay verified that Pt-1-treated cancer cells are immunogenic by showing a significantly delayed generation of tumours in the treatment group. Further *in vivo* study revealed that Pt-1 displayed a lower acute toxicity and stronger anti-tumour activity than oxaliplatin in the tumour-bearing immunocompetent mouse model in a manner associated with the activation of tumour immunity, rendering the Pt-aminophosphonate class of complexes a new scaffold for developing chemotherapeutics capable of triggering immune responses against solid tumours.

The Natural Science Foundation of China (No. 21401031, 21431001, 81473102), IRT\_16R15, Natural Science Foundation of Guangxi Province (No. 2015GXNSFAA139043, 2016GXNSFGA380005), the Fundamental Research Funds for the Central Universities, Guangdong Key Lab of Chiral Molecule and Drug Discovery (2019B030301005), and Shenzhen Fundamental Research Fund JCYJ20180508163206306 are acknowledged.

## Conflicts of interest

There are no conflicts to declare.

## References

- 1 Y. Jung and S. J. Lippard, *Chem. Rev.*, 2007, **107**, 1387–1407.
- 2 N. P. E. Barry and P. J. Sadler, *Pure Appl. Chem.*, 2014, **86**, 1897.
- 3 M. Fanelli, M. Formica, V. Fusi, L. Giorgi, M. Micheloni and P. Paoli, *Coord. Chem. Rev.*, 2016, **310**, 41–79.
- 4 N. Muhammad and Z. Guo, *Curr. Opin. Chem. Biol.*, 2014, **19**, 144–153.
- 5 M. A. Fuertes, C. Alonso and J. M. Pérez, *Chem. Rev.*, 2003, **103**, 645–662.
- 6 C.-H. Leung, S. Lin, H.-J. Zhong and D.-L. Ma, *Chem. Sci.*, 2015, **6**, 871–884.
- 7 A. Tesniere, F. Schlemmer, V. Boige, O. Kepp, I. Martins, F. Ghiringhelli, L. Aymeric, M. Michaud, L. Apetoh, L. Barault, J. Mendiboure, J. P. Pignon, V. Jooste, P. van Endert, M. Ducreux, L. Zitvogel, F. Piard and G. Kroemer, *Oncogene*, 2010, **29**, 482.
- 8 L. Galluzzi, A. Buqué, O. Kepp, L. Zitvogel and G. Kroemer, *Cancer Cell*, 2015, **28**, 690–714.
- 9 K. Lu, C. He and W. Lin, *J. Am. Chem. Soc.*, 2015, **137**, 7600–7603.
- 10 X. Zhao, K. Yang, R. Zhao, T. Ji, X. Wang, X. Yang, Y. Zhang, K. Cheng, S. Liu, J. Hao, H. Ren, K. W. Leong and G. Nie, *Biomaterials*, 2016, **102**, 187–197.
- 11 K. Lu, C. He, N. Guo, C. Chan, K. Ni, R. R. Weichselbaum and W. Lin, *J. Am. Chem. Soc.*, 2016, **138**, 12502–12510.
- 12 L. Zitvogel, O. Kepp and G. Kroemer, *Nat. Rev. Clin. Oncol.*, 2011, **8**, 151.
- 13 D. V. Krysko, A. D. Garg, A. Kaczmarek, O. Krysko, P. Agostinis and P. Vandenabeele, *Nat. Rev. Cancer*, 2012, **12**, 860.
- 14 I. Mellman, G. Coukos and G. Dranoff, *Nature*, 2011, **480**, 480.
- 15 N. Wang, Z. Wang, Z. Xu, X. Chen and G. Zhu, *Angew. Chem., Int. Ed.*, 2018, **57**, 3426–3430.
- 16 A. Terenzi, C. Pirker, B. K. Keppler and W. Berger, *J. Inorg. Biochem.*, 2016, **165**, 71–79.
- 17 U. Jungwirth, D. N. Xanthos, J. Gojo, A. K. Bytzek, W. Körner, P. Heffeter, S. A. Abramkin, M. A. Jakupec, C. G. Hartinger, U. Windberger, M. Galanski, B. K. Keppler and W. Berger, *Mol. Pharmacol.*, 2012, **81**, 719–728.
- 18 B. Englinger, C. Pirker, P. Heffeter, A. Terenzi, C. R. Kowol, B. K. Keppler and W. Berger, *Chem. Rev.*, 2019, **119**, 1519–1624.
- 19 D. Y. Q. Wong, W. W. F. Ong and W. H. Ang, *Angew. Chem., Int. Ed.*, 2015, **54**, 6483–6487.
- 20 D. Wernitznig, K. Kiakos, G. Del Favero, N. Harrer, H. Machat, A. Osswald, M. A. Jakupec, A. Wernitznig, W. Sommergruber and B. K. Keppler, *Metallomics*, 2019, **11**, 1044–1048.
- 21 M. Sabbatini, I. Zanellato, M. Ravera, E. Gabano, E. Perin, B. Rangone and D. Osella, *J. Med. Chem.*, 2019, **62**, 3395–3406.
- 22 M. Obeid, A. Tesniere, F. Ghiringhelli, G. M. Fimia, L. Apetoh, J.-L. Perfettini, M. Castedo, G. Mignot, T. Panaretakis, N. Casares, D. Métivier, N. Larochette, P. van Endert, F. Ciccosanti, M. Piacentini, L. Zitvogel and G. Kroemer, *Nat. Med.*, 2006, **13**, 54.
- 23 R. Tufi, T. Panaretakis, K. Bianchi, A. Criollo, B. Fazi, F. Di Sano, A. Tesniere, O. Kepp, P. Paterlini-Brechot, L. Zitvogel, M. Piacentini, G. Szabadkai and G. Kroemer, *Cell Death Differ.*, 2007, **15**, 274.
- 24 J. Krebs, L. B. Agellon and M. Michalak, *Biochem. Biophys. Res. Commun.*, 2015, **460**, 114–121.
- 25 Z. Xue, M. Lin, J. Zhu, J. Zhang, Y. Li and Z. Guo, *Chem. Commun.*, 2010, **46**, 1212–1214.
- 26 Y. Zhang, R. Cao, F. Yin, F. Y. Lin, H. Wang, K. Krysiak, J. H. No, D. Mukkamala, K. Houlihan, J. Li, C. T. Morita and E. Oldfield, *Angew. Chem., Int. Ed.*, 2010, **49**, 1136–1138.
- 27 M. Wilhelm, V. Kunzmann, S. Eckstein, P. Reimer, F. Weissinger, T. Ruediger and H.-P. Tony, *Blood*, 2003, **102**, 200–206.
- 28 Y. Xu, J. Aoki, K. Shimizu, M. Umezū-Goto, K. Hama, Y. Takanezawa, S. Yu, G. B. Mills, H. Arai, L. Qian and G. D. Prestwich, *J. Med. Chem.*, 2005, **48**, 3319–3327.
- 29 K. Becker, C. Herold-Mende, J. J. Park, G. Lowe and R. H. Schirmer, *J. Med. Chem.*, 2001, **44**, 2784–2792.
- 30 A.-B. Witte, K. Anestål, E. Jerremalm, H. Ehrsson and E. S. J. Arnér, *Free Radical Biol. Med.*, 2005, **39**, 696–703.
- 31 K.-B. Huang, Z.-F. Chen, Y.-C. Liu, Z.-Q. Li, J.-H. Wei, M. Wang, X.-L. Xie and H. Liang, *Eur. J. Med. Chem.*, 2013, **64**, 554–561.
- 32 K.-B. Huang, Z.-F. Chen, Y.-C. Liu, Z.-Q. Li, J.-H. Wei, M. Wang, G.-H. Zhang and H. Liang, *Eur. J. Med. Chem.*, 2013, **63**, 76–84.
- 33 The Pt compounds could react with DMSO and therefore the active species may be the DMSO adducts. Further studies are needed to verify this hypothesis.
- 34 N. Romani, S. Gruner, D. Brang, E. Kämpgen, A. Lenz, B. Trockenbacher, G. Konwalinka, P. O. Fritsch, R. M. Steinman and G. Schuler, *J. Exp. Med.*, 1994, **180**, 83–93.
- 35 A. A. van de Loosdrecht, E. Nennie, G. J. Ossenkoppele, R. H. Beelen and M. M. Langenhuijsen, *J. Immunol. Methods*, 1991, **141**, 15–22.
- 36 A. S. I. Loskog, M. E. Fransson and T. T. H. Totterman, *Clin. Cancer Res.*, 2005, **11**, 8816–8821.
- 37 S. Zhang, H. Xue and Q. Chen, *Oncotarget*, 2016, **7**, 58579–58585.